CHAPTER 5

THE SALT WEDGE

Harlow G. Farmer
Woods Hole Oceanographic Institution
Woods Hole, Massachusetts

George W. Morgan
Assistant Professor of Applied Mathematics
Brown University
Providence, Rhode Island

INTRODUCTION

The "salt wedge" is an idealized model of a phenomenon encountered in some estuaries. It consists of a layer of fresh river water flowing over and past an underlying layer of heavier salt water. The following study is an attempt to predict the shape of the salt wedge and its length measured from some significant point in the estuary in terms of quantities, such as the densities of the fresh and salt water, the average river depth and velocity, etc., which are usually available.

THEORETICAL ANALYSIS[2]

To simplify the mathematical treatment we assume that all variations in the direction of the estuary or channel width are negligible and that there is no velocity component in this direction. The channel has a plane horizontal bottom and its cross-section is rectangular and uniform.

We stipulate the existence of a sharp interface between the fresh water and the salt wedge, i.e., a density discontinuity, and the absence of mixing between the layers.

The equations of motion can then be written for each layer in the following form (Fig. 1):

---

[1]Contribution No. 638 from the Woods Hole Oceanographic Institution. This work was supported from funds made available by the Office of Naval Research, through their Contract No. N6onr-27701 (NR-083-004) with the Woods Hole Oceanographic Institution.

---

[2]For a more detailed account of the theory and additional investigations, see: L. Sanders, L. C. Maximon, G. W. Morgan, On the stationary "salt wedge" - a two layer free surface flow. Technical Report No. 1, Contract Nonr-56202 (NR-083-067). The theoretical results presented in this paper were obtained in the course of research sponsored by the Office of Naval Research under the above Contract with Brown University.

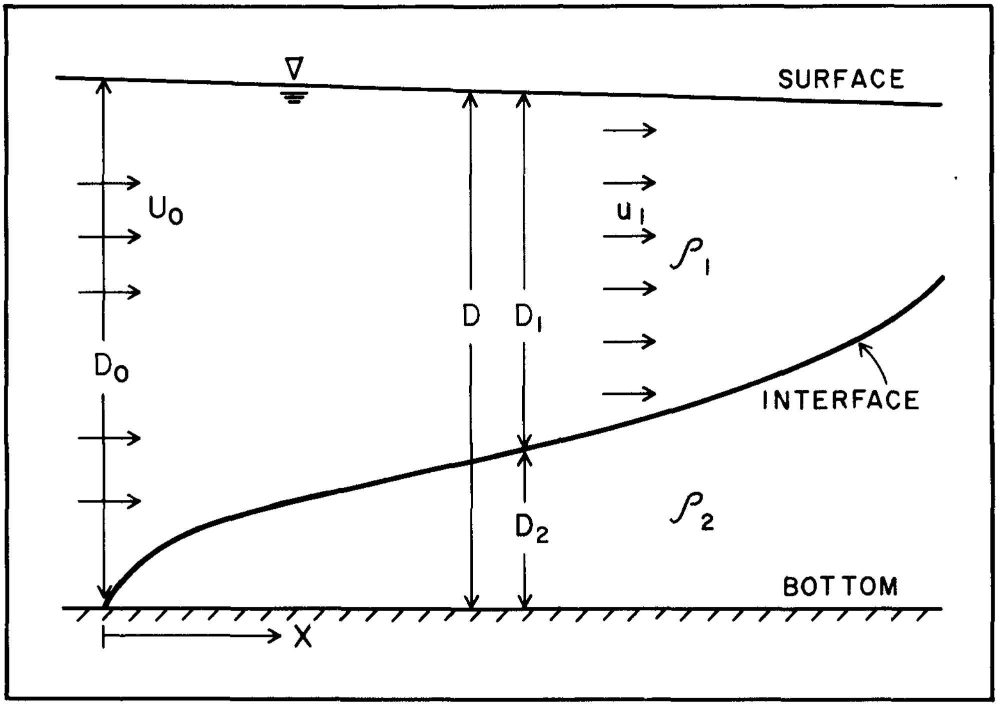

Fig. 1. Schematic diagram of salt wedge.

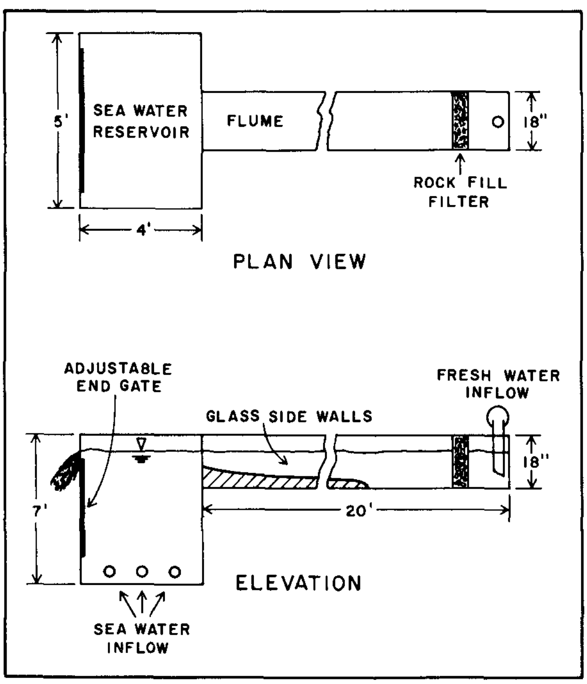

Fig. 2. Schematic diagram of
experimental apparatus.

$$\frac{\partial}{\partial x}(p_i + \rho_i u_i^2) + \frac{\partial}{\partial z}(\rho_i u_i w_i) = \frac{\partial}{\partial x}(A_i \frac{\partial u_i}{\partial x}) + \frac{\partial}{\partial z}(A_i \frac{\partial u_i}{\partial z}) \qquad (1)$$

$$\frac{\partial}{\partial z}(p_i + \rho_i w_i^2) + \frac{\partial}{\partial x}(\rho_i u_i w_i) = -\rho_i g + \frac{\partial}{\partial x}(A_i \frac{\partial w_i}{\partial x}) + \frac{\partial}{\partial z}(A_i \frac{\partial w_i}{\partial z}) \qquad (2)$$

$$\frac{\partial u_i}{\partial x} + \frac{\partial w_i}{\partial z} = 0 \qquad (3)$$

where the subscript i takes on the values 1 or 2 referring to the upper or lower layer, respectively;

- ρ is the density,
- p is the pressure,
- u is the horizontal velocity component,
- w is the vertical velocity component,
- g is the gravitational acceleration, and
- A is an eddy viscosity.

These equations apply to turbulent flow, the quantities u, w, p representing time averages of the actual time-dependent quantities.

If we neglect the inertia and shear forces in the vertical direction we can integrate the vertical momentum equation. Applying the condition $p = 0$ at the free surface $z = D$, we obtain

$$p_1 = \rho_1 g\,(D - z) \qquad (4)$$

and

$$p_2 = \rho_2 g\,(D_2 - z) + \rho_1 g D_1 \qquad (5)$$

where $z = D_2$ is the interface and $D_1 = D - D_2$, see Figure 1.

The solution is too difficult because of the presence of the unknown boundaries D, D_2. We therefore make a further approximation in our analysis by demanding that the laws of conservation of mass and momentum be satisfied only in the large rather than at every point of the flow, i.e., we integrate the equations over the depth. We then obtain the following equations from (1)

$$\rho_1 g D_1 \frac{d}{dx}(D_1 + D_2) + \rho_1 \frac{d}{dx}\int_{D_2}^{D} u_1^2\, dz = \tau_1 - \tau_2 \tag{6}$$

$$g D_2 \frac{d}{dx}(\rho_1 D_1 + \rho_2 D_2) + \rho_2 \frac{d}{dx}\int_{0}^{D_2} u_2^2\, dz = \tau_2 - \tau_0 \tag{7}$$

Here τ_0, τ_1, τ_2 are the values of $A \frac{\partial u}{\partial z}$ at $z = 0$, D, D_2 respectively, and we have neglected the term $\frac{\partial}{\partial x}(A \frac{\partial u}{\partial x})$ compared with $\frac{\partial}{\partial z}(A \frac{\partial u}{\partial z})$.

The continuity equation (3) gives

$$\frac{d}{dx}\int_{D_2}^{D} u_1 dz = 0 \tag{8}$$

or

$$\int_{D_2}^{D} u_1 dz = q \tag{8a}$$

and

$$\frac{d}{dx}\int_{0}^{D_2} u_2 dz = 0 \tag{9}$$

or

$$\int_{0}^{D_2} u_2 dz = 0 \tag{9a}$$

since there can be no net flow within the stationary wedge.

Equations (6) to (9) can now be treated in an approximate manner by assuming plausible velocity distributions u_1, u_2. Since the flow is turbulent it is reasonable to suppose that u_1 is fairly uniform over the depth except near the interface where sharp velocity gradients may be expected; i.e., $u_1 = \dfrac{q}{D_1}$. Since there is zero net flow across any section of the wedge and since the velocities in the wedge are caused by friction at the interface, we may expect that u_2 will be small compared with u_1 except possibly near the interface and that, therefore, the integral and the term τ_0 in equation (7), representing inertia forces and bottom shear forces, respectively, are negligible. We may also drop the free surface friction term τ_1.

We still know nothing concerning the nature of the interface shear force τ_2. At this point we content ourselves with developing a semi-empirical theory and take recourse to experimental results to determine an approximate law for τ_2.

It is convenient to rewrite equations 6, 7, 8a, 9a in non-dimensional terms by means of the following definitions:

$$D_1 = D_o n_1, \qquad D_2 = D_o n_2, \qquad z = D_o z', \qquad D = D_o D'$$

$$x = Lx', \qquad u_1 = U_o u_1', \qquad \tau_2 = \rho_2 U_o^2 \tau'$$

$$\beta = \frac{\rho_2 - \rho_1}{\rho_2}, \qquad \alpha = \frac{U_o^2}{g D_o \beta} \text{ and } \lambda = \frac{L}{D_o}$$

where D_o is a reference depth, taken to be the total depth at the tip of the wedge, L is the total length of the wedge, (to be defined later), and U_o is the uniform velocity of the fresh water at the tip of the wedge.

Incorporating the assumptions just discussed equations (6) and (7) become:

$$\frac{1-\beta}{\beta\alpha\lambda} n_1 \frac{d}{dx'}(n_1 + n_2) - \frac{(1-\beta)}{\lambda n_1^2}\frac{dn_1}{dx'} = -\tau' \tag{10}$$

$$\frac{1}{\beta\alpha\lambda} n_2 \frac{d}{dx'}\left[(1-\beta)\, n_1 + n_2\right] = \tau' \tag{11}$$

after putting

$$u_1' = \frac{1}{n_1} \tag{12}$$

To determine the shear law we insert observed values of n_1, n_2, etc. in equations (10) and (11) and calculate τ'.

The values of τ' found in this manner for various positions along a given wedge and for various wedges are found to be somewhat erratic, but it appears that over the range of α and β covered by our experiments τ' can be taken as approximately constant, say equal to K. This says that the shear force at the interface varies from wedge to wedge as the square of the fresh water velocity at the tip and is approximately constant over a given wedge.

Now, recalling that u_1' is constant with depth, equations (10) to (12) can be converted into the following two non-linear equations for the two unknowns n_1 and n_2.

$$(1-\beta)\, n_2\, (n_1^3 - \alpha)\, \frac{dn_1}{dx'} = -\lambda\alpha K n_1^2 \left[(1-\beta)\, n_1 + n_2\right] \qquad (13)$$

$$n_2 \frac{d}{dx'}\left[(1-\beta)\, n_1 + n_2\right] = \lambda\alpha\beta K \qquad (14)$$

To solve these we make use of the fact that β is very small (approximately 0.025) and develop n_1, n_2 in power series of β; i.e., we assume the following forms of solutions:

$$n_1 = n_{10} + \beta n_{11} + \beta^2 n_{12} + \ldots \qquad (15)$$

$$n_2 = n_{20} + \beta n_{21} + \beta^2 n_{22} + \ldots \qquad (16)$$

For small β we may hope that n_1, n_2 will be given sufficiently accurately by the first term of the power series.

Inserting the series into equations (13) and (14) and equating the coefficients of like powers of β we obtain as the equations to be satisfied by n_{10} and n_{20}:

$$n_{20}\, (n_{10}^3 - \alpha)\, \frac{dn_{10}}{dx'} = -\lambda\alpha K n_{10}^2\, (n_{10} + n_{20}) \qquad (17)$$

$$n_{20} \frac{d}{dx'} (n_{10} + n_{20}) = 0 \qquad (18)$$

If we take the origin $x = 0$ at the tip of the wedge, our boundary conditions are

$$n_{10}(0) = 1 , \qquad\qquad n_{20}(0) = 0 \tag{19}$$

Equation (18) gives

$$n_{10} = 1 - n_{20} \tag{20}$$

and then (17) becomes

$$n_{20}\left[(1 - n_{20})^3 - \alpha\right] \frac{dn_{20}}{dx'} = \lambda K \alpha (1 - n_{20})^2 \tag{21}$$

Equation (21) can be integrated to give

$$\lambda \alpha K x' = \frac{1}{6} n_{20}^2 (3 - 2n_{20}) - \alpha \left[\frac{n_{20}}{1 - n_{20}} + \log (1 - n_{20})\right] \tag{22}$$

The left-hand side of equation (22) is $\alpha K \frac{x}{D_o}$. Hence, provided K can be found, and presuming α is given, equation (22) is an expression for the shape of the wedge. The value of K must be found by observing n_{20} for one or more experiments and calculating K from the equation (22) for these experiments.

So far we have no information concerning λ , the length of the wedge in fact this length is not yet defined. In the experimental set-up the channel leads to a reservoir which represents the ocean and the transition section from channel to reservoir determines the location of the wedge. We therefore define the length of the wedge to be the distance from the wedge tip to the reservoir. Experimentally the slope of the interface is found to be very large near the tip, to decrease with increasing x and the to increase again as the reservoir is approached. It is also observed tha $\frac{n_1^3}{\alpha}$, which equals $\frac{gD_1^3\beta}{q^2}$, approaches unity as one approaches the reservoir.

Equation (21) shows that the slope of the interface is infinite at the tip and again when $(1 - n_{20})^3 = \alpha$ or when

$$\frac{n_{10}^{3}}{\alpha} = 1. \qquad (23)^{3}$$

We cannot, of course, expect our equations to hold near these regions, but, in order to obtain an estimate of the length of the wedge we formally associate the point at which $\frac{n_{10}^{3}}{\alpha} = 1$ with the section of transition to the reservoir. Hence the depth of the wedge at the reservoir, say n_{20}^{*}, is given by

$$n_{20}\,(1) = n_{20}^{*} = 1 - \sqrt[3]{\alpha} \qquad (24)$$

Substituting $n_{20} = n_{20}^{*}$ and $x' = 1$ into equation (22), we obtain a formula for λ in terms of n_{20}^{*} :

$$\lambda K \alpha = \frac{1}{6}\,(n_{20}^{*})^{2}\,(3 - 2n_{20}^{*}) - \alpha \left[\frac{n_{20}^{*}}{1 - n_{20}^{*}} + \log\,(1 - n_{20}^{*})\right] \qquad (25)$$

Equation (25) together with equation (24) provides an alternate method of finding K by measuring λ for one or more experiments.

A convenient method of comparison between theory and experiment is afforded by plotting $\frac{n_{20}}{n_{20}^{*}}$ against x'. The theoretical curves are found to be practically independent of α for all permissible values of α, i.e., for α ranging between zero and one. They are approximately given by

$$x' = \left(\frac{n_{20}}{n_{20}^{*}}\right)^{2}\left(3 - 2\,\frac{n_{20}}{n_{20}^{*}}\right) \qquad (26)$$

If one wishes to apply the theory to actual estuaries where the values of U_0 and D_0 differ drastically from those in the experimental set-up, it is necessary to first obtain a value of K from observation. Inasmuch as K is a kind of measure of the turbulent shear at the interface its value will be different for various estuaries and, of course, will be different from that in the experimental set-up. It may be hoped, however,

[3] For a separate discussion of this criterion at transitions see Stommel and Farmer, 1952.

that the value of K will remain reasonably constant for a given experimental set-up or estuary although U_o, D_o, β may vary.

EXPERIMENTATION

Figure 2 shows in outline form the experimental apparatus used in the salt wedge studies. The flume has plate glass side walls and a level bottom. The reservoir and flume are connected together through a six inch long elliptically shaped transition. The total depth of water in the reservoir and flume is controlled by the weir on the overflow side of the reservoir. The concrete reservoir, representing the ocean source in the apparatus, is constantly supplied with sea water. The salinity of the sea water remains at a satisfactorily constant 32 $^o/oo$ and the density is determined from its temperature and salinity. Fresh water is metered with a Rotometer before discharging into the upstream end of the flume. In order to vary the density difference of the two waters in the flume, sea water may be drawn from the concrete reservoir source, separately metered, and then mixed with the fresh water before discharging into the flume. The specific gravity of the fresh and salt water mixtures was taken by hydrometer, and these values were used as density. The wedge profiles were measured with point gauges, the level of the interface being taken in the troughs of the internal waves which were present at the interface.

A total of 45 different salt wedges was established in the flume, β being held a constant 0.025 for 27 runs, and in the remaining 18 it was varied from 0.0170 to 0.000684. A full account of the experimental data is given by Farmer, 1951.

DISCUSSION OF RESULTS

Figure 3 shows the approximate theoretical curve for the shape of the wedge as given by equation (26), as well as one set each of experimental data from the flume and observational results, Rhodes, 1950, from the Mississippi River South West Pass.

Figure 4 is a typical curve of dimensionless length $\lambda = \frac{L}{D_o}$ versus discharge q for a given density difference β and a fixed K and D_o, the values chosen being of the order of magnitude pertinent to the Mississippi River. The value K = .001 was determined for the salt wedge in South West Pass, D_o = 48 ft., q = 66 ft^2/sec., L = 10 miles and β = .0196. D_o was taken as the total depth at the tip of the wedge.

Figure 5 shows the variation of λ with β for a fixed value of $\frac{U_o^2}{gD_o}$ and K.

Comparison of theory with experimental results based on K = 0.006 gives fairly good agreement for the interface shape. Theoretical predictions of the length of the wedges agree with experiment to within approximately 15%.

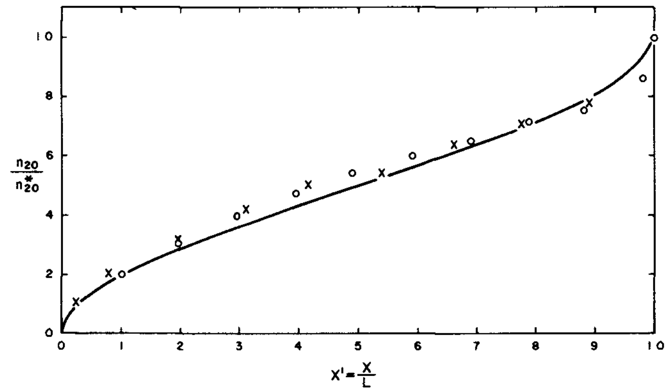

Fig. 3. Non-dimensional shape of salt wedge; the solid line is given by Equation (26), O's refer to Mississippi River South West Pass and x's refer to experimental run A-8.

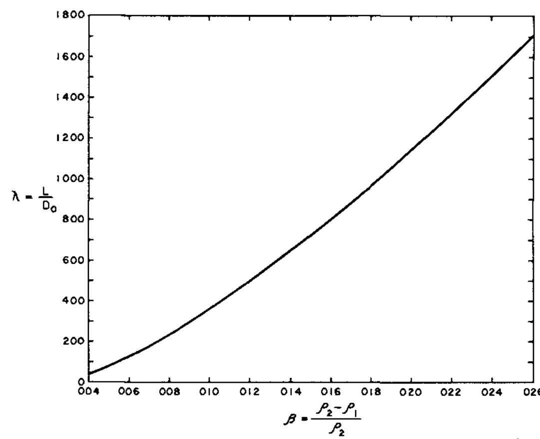

Fig. 5. Non-dimensional length L/D_o

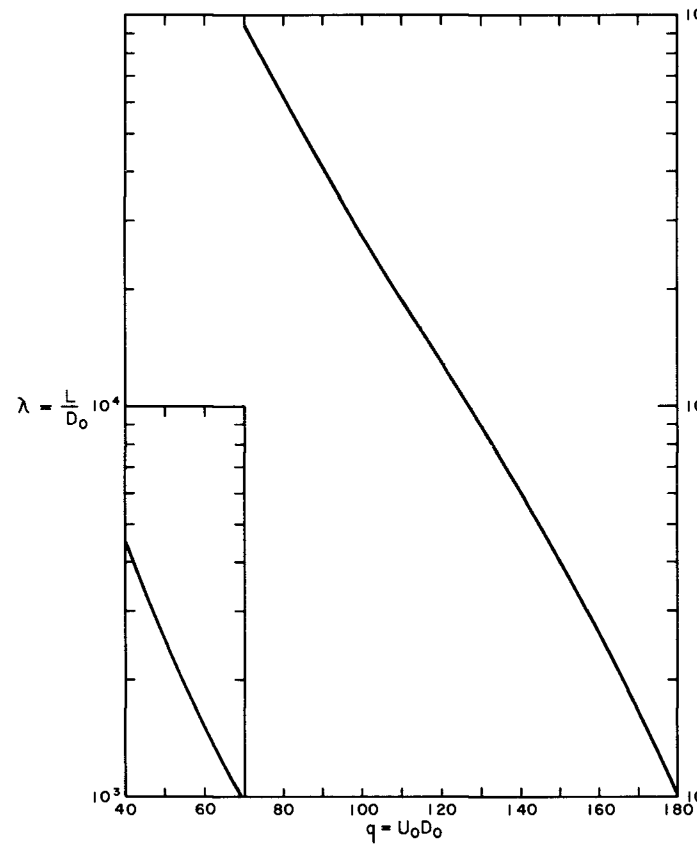

Fig. 4. Non-dimensional length L/D_o versus discharge per unit width q. D_o = 48 ft., β = .0196, and K = .001.

Observational data were limited to a few isolated curves for the Mississippi River. In this connection it must be pointed out that in the range of α encountered in the Mississippi the length, as predicted by theory, is very sensitive to slight changes in river depth D_0. Since the bottom is not horizontal, the question of what value of D_0 to choose in attempting to apply the theory becomes a difficult one and will require further study.

REFERENCES

Farmer, Harlow G. (1951). An experimental study of salt wedges: Woods Hole Oceanographic Institution Technical Report, Reference No. 51-99, Manuscript Report to Office of Naval Research.

Rhodes, Ralph F. (1950). Effect of salinity on current velocities: Committee on Tidal Hydraulics, Report No. 1, Corps of Engineers, U. S. Army.

Stommel, Henry and Farmer, H. G. (1952). Abrupt change in width in two layer open channel flow: J. Mar. Res. XI (2), 205-214.